

Molecular Dynamics Study of the Effect of Layer Charge and Interlayer Cations on Swelling of Mixed-Layer Chlorite–Montmorillonite Clays

Mahsa Rahmostaqim and Muhammad Sahimi*

Cite This: <https://dx.doi.org/10.1021/acs.jpcc.9b10919>

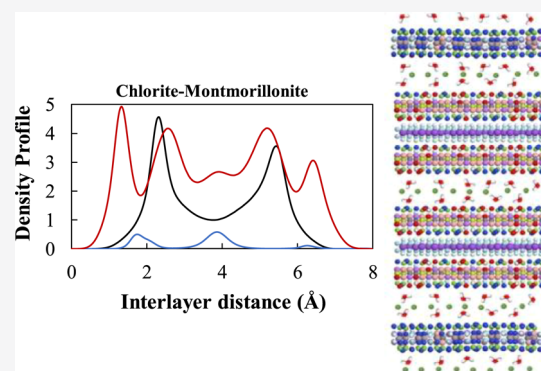
Read Online

ACCESS |

Metrics & More

Article Recommendations

ABSTRACT: Understanding the properties of clay minerals is crucial to various phenomena in geophysics and environmental science and engineering. Although about 70 percent of all clays are of mixed-layer (ML) types, such as illite-montmorillonite (I-MMT) and chlorite–montmorillonite (CH–MMT) clays, the vast majority of the previous experimental and simulation studies were focused on pure clays. This paper reports on a study of important properties of ML clays by molecular dynamics simulations. One goal of the study is to understand the differences between the behavior of CH–MMT and pure chlorite and MMT. Another goal is to understand the effect of cations on the swelling behavior of the ML clays, for which we use Na^+ , K^+ , and Cs^+ . In both CH–CH and CH–MMT, the strong octahedral substitution of the chlorite layer results in, respectively, increasing both polarization and adsorption of water near, and onto the clay surface. The latter reduces hydration of the interlayer cations and, consequently, swelling of the CH–CH and CH–MMT clays, a conclusion that is supported by the computed density profiles and the radial distribution functions. Compared with the octahedral substitutions, the interlayer cation concentration and tetrahedral substitutions are shown to have a substantially weaker effect on swelling, whose pattern is also a function of the type of the interlayer cation. We find that the differences in the size and hydration energy of the cations have strong implications for the distribution of the interlayer species and, thus, their swelling, and that the higher the hydration energy and the smaller the atomic radius of the cation, the more swelling of the clay interlayers occurs. We also show that the layer substitution, the location, density, type of interlayer cations, and asymmetry of the ML clays play important roles in swelling of ML clays.



1. INTRODUCTION

Understanding swelling of sedimentary rock, and in particular its clay minerals, in the presence of water or/and CO_2 is critical for many environmental and industrial processes. A key role of the clays is limiting leakage and transport of contaminants in the subsurface^{1–3} and, therefore, how they may swell and allow more leaking of contaminants is an important problem that has been studied for a long time.

Swelling of clays occurs by two distinct mechanisms, namely, crystalline and osmotic swelling.⁴ Crystalline swelling occurs with water adsorption in the interlayer and by a stepwise mechanism,^{5–8} with the layer spacing reaching the equilibrium state when the total free energy of the system is minimum. The typical crystalline basal spacing ranges from 9 to 20 Å. Osmotic swelling, on the other hand, occurs in some specific clays in which water molecules are drawn to the interlayer from the surrounding, with the typical interlayer spacing being anywhere from 20 to 130 Å. Sodium-smectites tend to swell up by the osmotic mechanism, whereas potassium-smectites swell in

crystalline hydrate form, which is why potassium is used to limit swelling of sodium-saturated clays.^{9,10}

Most of the previous studies of swelling of clays focused on pure ones, especially the montmorillonite (MMT) clays. Liu and Lu studied^{10,11} inhibition of clay swelling by potassium ions, and reported that global minimum energy of K-smectites is reached in a single-layer hydrated state, whereas Na-smectites reach their global minimum energy in the double-layer state. Therefore, it is energetically favorable for Na-smectites to swell, whereas potassium limits swelling of the smectites. In a similar study by Smith,¹² swelling properties of cesium–MMT were investigated. Similar to potassium, cesium manifests a distinct plateau of layer-spacing at the monolayer hydrate spacing where the global minimum energy occurs. The

Received: November 21, 2019

Revised: December 23, 2019

Published: January 3, 2020

higher the hydration energy, the more swelling may be expected.

Thus, these studies indicate that the type, charge, and size of the interlayer cations greatly affect clay swelling. Mooney et al. compared¹³ by experiments swelling in the presence of Na^+ , Rb^+ , Cs^+ , K^+ , and Li^+ and reported that as the cation's atomic radius increases, less water is adsorbed in the interlayer and, therefore, less swelling occurs. Clay swelling is also correlated with the hydration energy of the cations. The higher the hydration energy, the more swelling is expected.^{14,15} In addition to the ion type, layer substitution plays an important role in swelling characteristics of clay minerals. In two studies,^{7,16} two MMT clays, one with both octahedral and tetrahedral substitution and a second one with only octahedral substitution, were considered. Under the same conditions, a smaller extent of swelling was observed for the MMT with both octahedral and tetrahedral substitutions.

Smith et al.¹⁷ explored the effect of a range of octahedral layer charges on swelling of Na-MMT, and demonstrated that increased layer charge results in more swelling. In a separate study by Whitley and Smith,¹⁸ the increase in the layer charge affected swelling similar to the increase in the hydration energy of the interlayer cations. In an experimental study, Foster¹⁹ investigated the relationship between ionic substitution and swelling of the MMT. He found that the increase in the octahedral substitution reduces swelling of the MMT. He also considered the effect of the number of cations in the interlayer as well as tetrahedral substitution in clay swelling, but reported that the two factors had little or no effect on swelling, whereas octahedral substitution plays a significant role in the swelling volume of the MMT.

These studies were focused on pure clays. Mixed-layer (ML) clays form, however, in abundance and in many varieties in sedimentary rocks. In fact, a study of more than 6000 sedimentary rock samples in the United States indicated²⁰ that more than 70 percent of them contained some form of ML clays. Thus, it is far more likely to find ML illite-MMT (I-MMT) and chlorite-MMT (CH-MMT) than pure clays because of the transformation of the latter by marine diagenesis and weathering. Among the wide range of combinations of clays in the ML form, the most common types are I-MMT, I-CH, CH-MMT, and I-CH-MMT clays.

In two previous papers,^{21,22} we reported the results of our molecular simulation studies of swelling of the I-MMT clays in the presence of water, water and CO_2 , and two different interlayer cations. Our studies indicated significant differences between the properties of pure and ML clays in contact with various combinations of the interlayer species. In the present paper, we report the results of our molecular simulation study of the same problems in another type of ML clays, namely, the CH-MMT clays, which represent the second most common type of such clays.²³ This type of the ML clays is formed when $\text{Mg}(\text{OH})_2$ replaces interlayer cations and water in the MMT. In the conversion of smectites to chlorites, the brucite layer, generated by polymerization of the existing complex ions in sedimentary rock, locks together the two 2:1 sheets of converted smectite and forms a nonexpandable 2:1:1 clay.²⁴ In the CH-MMT mixed clays, however, the space between the 2:1:1 chlorite and the adjacent MMT and the chlorite layers can swell during hydration. The structure of both chlorite and MMT clay layers consists of a 2:1 or tetrahedral–octahedral–tetrahedral–octahedral (TOT) structure. In most of the ML CH-MMT layers, the chlorite clays are trioctahedral, whereas

the MMT is dioctahedral. In the trioctahedral phyllosilicates structure of chlorite, the octahedral layers are similar to brucite, with Mg^{2+} or Fe^{2+} occupying the cation positions. On the other hand, in dioctahedral phyllosilicates of the MMT, the octahedral layers are similar to gibbsite, with Al^{3+} occupying those positions. A chemical analysis of some of the ML CH-MMT samples are presented by Weaver and Pollard.²⁵ In both types of clays, the negative charge of the TOT layer is balanced by the interlayer cations, such as Na^+ , Ca^{2+} , Cs^+ , and K^+ . Such cations, in the presence of water, are usually hydrated, resulting in swelling of the clays.²⁶ The extent of swelling depends, however, on the cation type,^{5,13} the humidity, clay type, and the charge distribution^{27–29} in the clay structure.

Computational studies, and in particular molecular dynamics (MD) simulation, are highly useful for gaining a deep understanding of the molecular origin of many phenomena, and in particular swelling of clays. Thus, MD simulations are being increasingly used for obtaining information about clay swelling at molecular scales, as they represent an economical and efficient way of studying such complex problems. Advances in computational resources provide the ability for investigating swelling of the more common types of clays, namely, the ML clays, and computing their properties at the molecular scale. Among such simulations, the study by Teich-McGoldrick et al.³⁰ focused on a comparison of swelling properties of the MMT and beidellite as a function of the temperature, interlayer cation, layer charge, and charge location. They did not, however, consider the ML MMT–beidellite interlayer, and focus instead on comparing the properties of the MMT–MMT and beidellite–beidellite interlayer.

In the present paper, we focus on ML CH-MMT clays, and report on the results of extensive MD simulation of swelling of three distinct interlayers, namely, CH-CH, MMT-MMT, and CH-MMT, in contact with a range of water concentrations, and as a function of the interlayer cation, Na^+ , K^+ , and Cs^+ . The results for the MMT-MMT interlayer are used as a reference to compare with the other cases.

The organization of the rest of the paper is as follows. We first describe the methodology and computational procedure for the MD simulations. The results are then presented and discussed in Section 3, and the paper is summarized in the last section.

2. COMPUTATIONAL DETAILS

The chlorite structure that we simulate in this study was inspired by the work of Meunier et al.²⁴ who studied the smectite-to-chlorite conversion. In the conversion process, saponite and chlorite interact, resulting in the formation of a structure that has the properties of saponite on one side and those of chlorite on the other side in each layer. The supercell structure that we utilized in the MD simulations contained four orthogonal clay layers consisting of two chlorite and two MMT layers with the arrangement, MMT-CH-CH-MMT. The snapshot of the dry supercell structure is presented in Figure 1. Each of the layers contained 25×4 unit cells, arranged along the (xy) directions (see Figure 1), with the supercell containing 80 unit cells in a $5 \times 4 \times 4$ arrangement. As mentioned in the Introduction, each chlorite layer consists of two 2:1-type layers along with a central brucite-like layer, which is why chlorite is sometimes called 2:1:1 clay mineral. Each of the 2:1 layered chlorite has an asymmetric structure, generated as a result of the interactions between saponite and

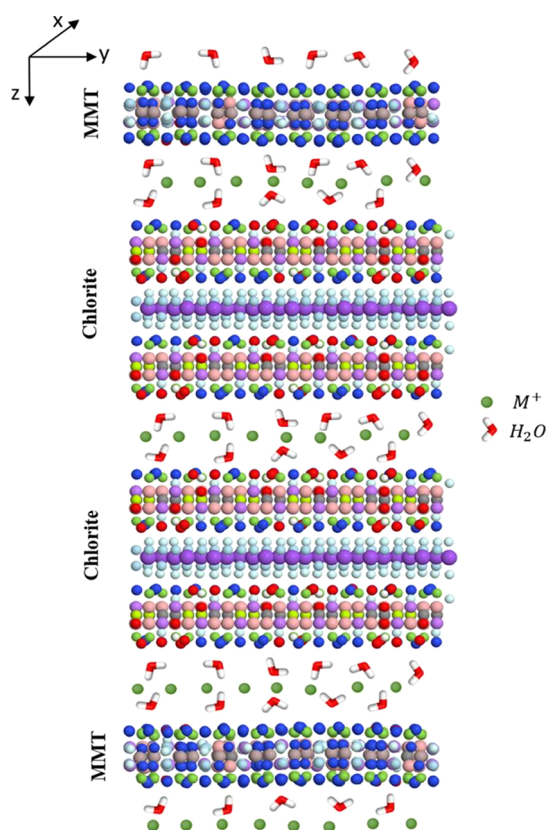


Figure 1. Schematic side view of the simulation cell for the CH–MMT ML clay. M^+ represents the interlayer cation.

chlorite with the composition $M_{0.53}^+[(Si_{3.35}Al_{0.65})(Si_{2.9}Al_{1.1})]_2O_{20}R_6^{2+}(OH)_4 \cdot nH_2O$, where $R_6^{2+} = Fe_3^{2+} + Mg_3^{2+}$, and $M_{0.53}^+$ is the interlayer cation. The brackets enclose the atoms in the tetrahedral sheet, whereas the parenthesis inside the brackets indicate the asymmetric structure of the tetrahedral layer. Because of asymmetry of each 2:1 sublayer of chlorite, and in order to keep the CH–CH interlayer symmetric, the $Si_{2.9}Al_{1.1}$ sides of the two CH sublayers face the brucite-like layer, whereas the $Si_{3.35}Al_{0.65}$ sides face the interlayer species in both CH–CH and CH–MMT interlayers. Three cations, Na^+ , Cs^+ , and K^+ , were used in the MD simulations in order to understand their effect on swelling of the clays. The number of water molecules n was increased monotonically in each set of simulations. The composition of the brucite layer between the two 2:1 layers of chlorite was $Mg_3(OH)_6$. The MMT was the same as what we used in our previous studies,^{21,22} with its chemical composition being $Na_{0.75}Si_{7.75}Al_{0.25}Al_{3.5}Mg_{0.5}O_{20}(OH)_4 \cdot nH_2O$. The lateral (x, y) dimensions (see Figure 1) of each individual clay layer under dry conditions were approximately $26 \times 36 \text{ \AA}$, and the substitutions in each layer were distributed symmetrically. The cations M^+ were distributed in the interlayer of the CH–CH, CH–MMT, and MMT–MMT, in order to balance the negative charge of the clay sheets.

The MD simulations were carried out using the LAMMPS (Large-scale Atomic/Molecular Massively Parallel Simulator)³¹ simulation package. The clay structure was described by the CLAYFF force field,³² and the interlayer water molecules were modeled by the flexible SPC model. The charges assigned to each atom were according to the CLAYFF table. Periodic boundary conditions were imposed in all

directions, and the system could freely expand or shrink perpendicular to the clay layers along the z axis shown in Figure 1. Note that each of the clay layers—the 2:1 structure for each MMT layer and the 2:1:1 structure for each chlorite layer—is allowed to move as individual units and only along the Z axis. The interlayer species (water and the interlayer cations) are, however, free to both translate and rotate inside the interlayers.

The dry system was first equilibrated employing the isobaric-isothermal ensemble (NPT) with $T = 348 \text{ K}$ and $P = 130 \text{ bar}$, which are close to the conditions in geological cap rock. After equilibration, the dry basal spacings d were calculated. Next, for all the independent cases with various water concentrations, MD simulations in the NPT ensemble were carried out with a time step of 0.01 fs , which was gradually increased to 1 fs and were continued for at least 20 ns . Longer simulations were carried out for higher water concentrations until equilibrium was reached. Temperature was controlled by a Nose–Hoover thermostat, with the coupling constants being 100 and 1000 timesteps, respectively. The short-range interactions above 13 \AA were truncated, whereas the long-range electrostatic interactions were calculated employing the particle-mesh Ewald summation with an accuracy of 10^{-4} . For each case, the basal spacings were computed at the end of each series of the MD simulation. The equilibrated states obtained by the simulation in the NPT ensemble were then used as the input for the simulations in the canonical (NVT) ensemble, which were carried for up to 20 ns for the cases with higher water concentrations. Note that in each ensemble, the equilibrium state of the system was considered reached when the thermodynamic potential of the system was at its minimum for the given temperature and pressure of the ensemble. The results obtained with the NVT ensemble were used to compute the density profiles as well as the radial distribution functions (RDFs).

Independent simulations were also carried out for several water contents in each interlayer, which was increased from 1 to 10 molecules per unit cell, in order to monitor the one-layer (1W) and two-layer (2W) hydration of the clays. Each hydration layer of water refers to the number of distinct water layers inside the clay interlayer, which are formed by the gained water in the hydration shell of the interlayer cations. The 1W and 2W hydration states are shown and discussed in the section below on the results for the density distribution profiles, with one and two distinct water oxygens, respectively.

Therefore, a total of 30 cases were simulated in this study, and the results for the three different interlayers were compared. In all the simulations, the water molecules were randomly distributed in the interlayer, whereas the cations were initially distributed in the midplane of the interlayers.

3. RESULTS AND DISCUSSION

In what follows, we present and discuss some important properties of the clay to better understand the reason for observed behaviors of the swelling clay under different conditions.

3.1. Swelling. Figures 2 and 3 present the basal spacing d for all the cases that we simulated, which, for the sake of clarity and better understanding of the factors that influence swelling, are grouped based on the interlayer cations. As the thickness of chlorite and the MMT layers are dramatically different, the basal spacing for all the interlayers, including the CH–CH interlayer, were calculated as the sum of thickness of the MMT

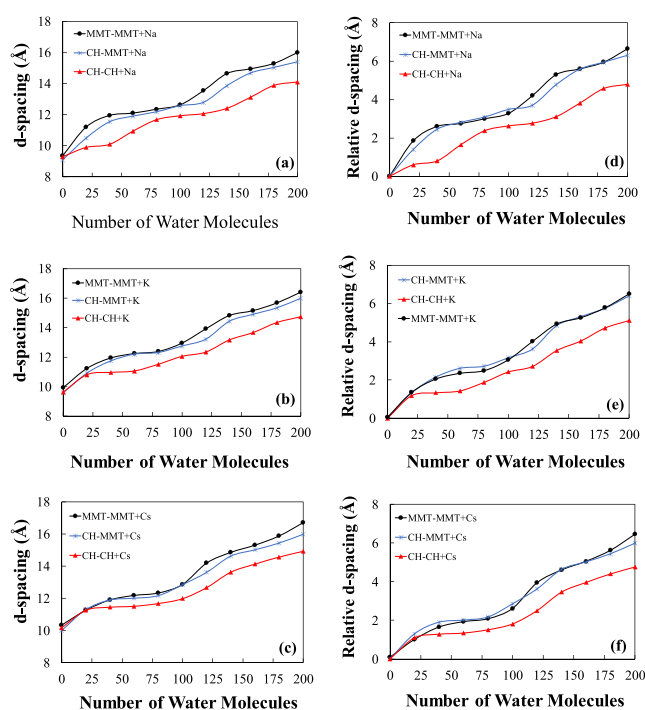


Figure 2. Comparison of the absolute (a–c) and relative (d–f) basal spacing of the clay interlayers as a function of interlayer cation and the water content, grouped by the cation type.

clay and the interlayer distance. Computed in this way, the comparison of the amount of swelling will be independent of the clay thicknesses and depends only on the extent of expansion or compression of the interlayer space.

Figure 2a–c shows the absolute basal spacing of the three interlayers at various water concentrations. To be able to compare the results for the three interlayers, Figure 2d–f presents the basal spacing of the clay interlayers relative to their corresponding dry states. They demonstrate that swelling of the MMT–MMT interlayer and the CH–MMT mixed interlayers are, relatively speaking, similar. For all the three cations, Na⁺, K⁺, and Cs⁺, the CH–CH interlayer has a significantly different basal spacing and lower extent of swelling.

In addition, a few points are worth pointing out. (i) For the cases in which sodium acts as the cation in both CH–MMT and CH–CH interlayers, the transition to the first and second hydration states is postponed to higher water contents. The delay is very significant for the CH–CH interlayer. (ii) When potassium is the interlayers' cation, the clay expansion occurs more monotonically, when compared with sodium. As a result, the transitions between the hydration states take place

smoother and at similar water contents, with no obvious delays for the CH–CH interlayer. (iii) The cesium clay exhibits a significantly different swelling behavior with a wide first-layer hydration state that persists up to the water content of 100 molecules, which is consistent with the experimental results in the literature. According to Smith,¹² the potential energy of cesium clay reaches its global minimum in the monolayer hydrate.

This result for the symmetric interlayers, that is, the CH–CH and MMT–MMT interlayers, is interpreted by the differences in the hydration enthalpy of the interlayer ions and the layer substitutions in the clay. For the asymmetric interlayer—the CH–MMT mixed clay—in addition to the aforementioned factor, the different structures of the clay surfaces that are in contact with the interlayer species play an important role in the observed differences. Na⁺, K⁺, and Cs⁺ have hydration enthalpies of −406, −320, and −264 kJ/mol, respectively. The hydration enthalpy affects the interaction of the cation and the clay surface and, as it decreases, so also does the amount of clay swelling. This is why K⁺ is used as the water network breaker in order to control swelling of smectite clays.^{10,33,34} Therefore, the larger and weakly hydrating ions have lower amounts of water in their hydration shells and, therefore, a lower extent of swelling.

Moreover, the amount and the location of the substitutions explain the differences in the amount of swelling for each specific ion. The main difference between the structures of the MMT and CH is the full substitution of Al³⁺ with Mg²⁺ and Fe²⁺ in the octahedral layer of CH. It has been reported¹⁹ that Fe²⁺ in the octahedral sheet has a great suppressing effect on the swelling volume of the MMT, which is similar to Mg²⁺. Moreover, the tetrahedral substitution of the tetrahedral sheet of the CH facing the interlayer species is considerably higher than that of MMT. This can be better understood by comparing the tetrahedral structures of the two, Si_{3.35}Al_{0.65} and Si_{3.875}Al_{0.125}, which refer, respectively, to the CH and MMT tetrahedral sheets facing the clay interlayer. The comparison clearly indicates 5.2 times more substitution of Si⁴⁺ with Al³⁺ in the CH tetrahedral sheet, when compared with the MMT.

Figure 3 groups the relative swelling curves by the interlayer type in order to explore independently the effect of the ion type on swelling. Figure 3a indicates that in the MMT–MMT interlayer, the overall transitions of the swelling curves are similar, except for the fact that as the hydration enthalpy of the ion decreases and the ion radius increases, the amount of swelling decreases, and the transitions are postponed to higher water contents. Figure 3b indicates behavior more similar to that shown in Figure 3a than to Figure 3c, hence demonstrating that the MMT side of the CH–MMT interlayer

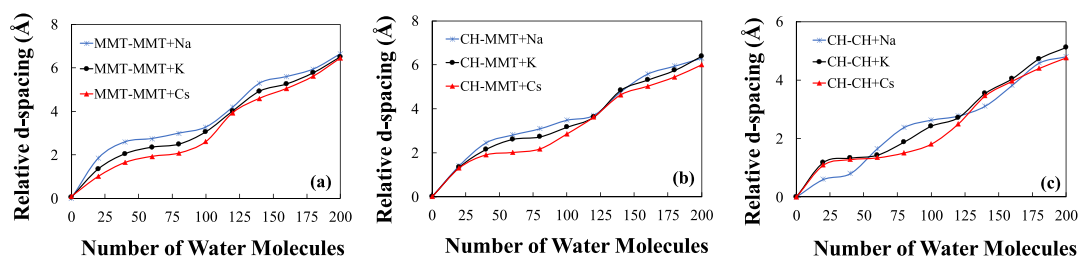


Figure 3. Comparison of the absolute basal spacing of the clay interlayers as a function of interlayer cation and the water content, grouped by the interlayer type. (a) MMT–MMT; (b) CH–MMT + cation, and (c) CH–CH, all plus the cation.

contributes effectively to the clay swelling more than the CH side. Figure 3c, on the other hand, presents an interesting behavior. The Cs–CH–CH system indicates the widest monolayer, when compared with all other cases that we have considered. Although swelling of Na–CH–CH is considerably lower than the other two interlayers, it still exhibits two distinct layers that are, however, unstable, having a short interval of hydration for a monolayer with an early transition to the bilayer. Finally, the K–CH–CH depicts something in between the other two cases, which is consistent with the hydration enthalpy of K and its ion size, when compared to the other two ions. The swelling is also monotonic.

These results show that the CH–CH interlayer is more sensitive to the interlayer cation than are the other two interlayers, hence implying that the octahedral substitutions are more responsive to the ion type than the tetrahedral substitutions. It should be mentioned that our results for swelling of the MMT–MMT interlayer are consistent with the existing results in the literature,^{7,34–37} and are used for validating the simulations. We also note that the CLAYFF overestimates the surface–ion interactions for the surface oxygen. This results in some extra inner-sphere surface complexes of the ions and the surface and, thus, a slightly smaller extent of swelling than the experimental data.

3.2. Molecular Structure of the Interlayers. The results for the basal spacings can be better understood by comparing the density profiles of the various cases that we have studied. Figures 4–6 present density profiles of the 1W and 2W

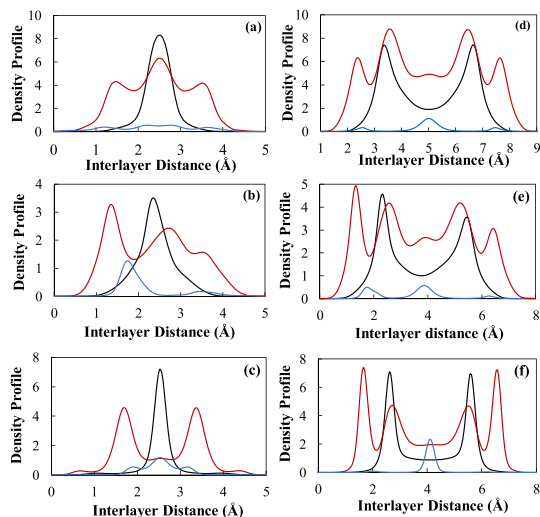


Figure 4. Density profiles of (a–c) the 1W and (d–f) 2W hydration states perpendicular to the clay surface for Na plus (a,d) MMT–MMT; (b,e) CH–MMT, and (c,f) CH–CH. In the CH–MMT interlayer, the left and right surfaces are CH and MMT, respectively. Water oxygen and hydrogen are represented by black and red, and Na⁺ by blue.

hydration states in the interlayer region along the *z* direction, perpendicular to the clay surface, in the presence of the three cations. The results are for the cases in which the water content was fixed at 60 molecules per interlayer for the monolayer and 180 molecules per interlayer for the bilayer hydration states (three and nine molecules per unit cell, respectively). This was done in order to make the comparison at a fixed water concentration for all the interlayers. The computed density profiles for the MMT–MMT interlayers

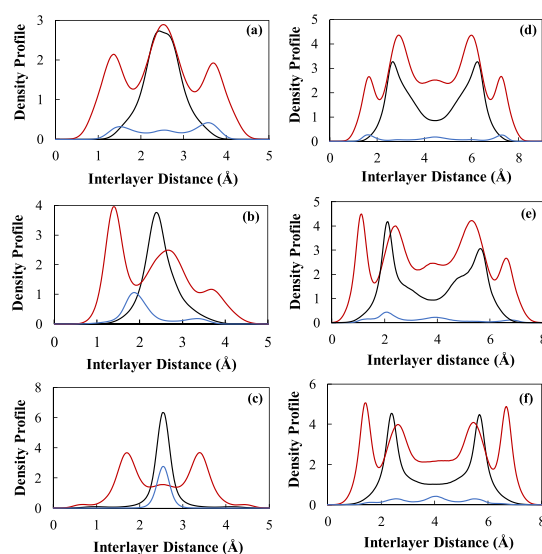


Figure 5. Density profiles of the 1W (a–c) and 2W (d–f) hydration states perpendicular to the clay surface for K plus (a,d) MMT–MMT; (b,e) CH–MMT, and (c,f) CH–CH. For the CH–MMT interlayer, the left and right surfaces are CH and MMT, respectively. Water oxygen and hydrogen are represented by black and red, and K⁺ by blue.

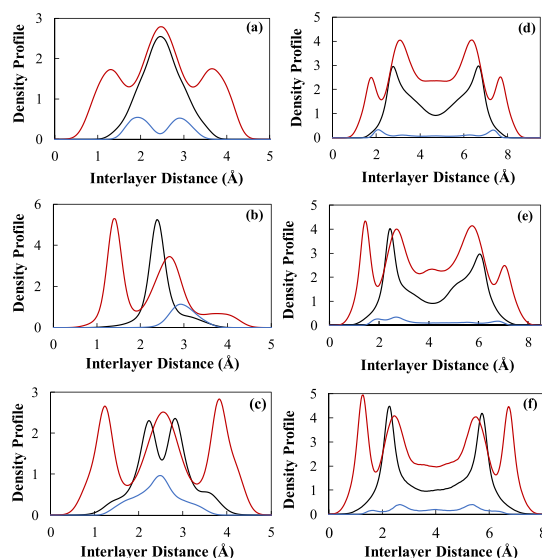


Figure 6. Density profile of the 1W (a–c) and 2W (d–f) hydration states perpendicular to the clay surface for Cs plus (a,d) MMT–MMT; (b,e) CH–MMT, and (c,f) CH–CH. In the CH–MMT interlayer, the left and right surfaces are CH and MMT, respectively. Water oxygen and hydrogen are represented by black and red, and Cs⁺ by blue.

agree well with the previous studies of 1W and 2W hydration states.^{30,35,37} However, a few variables must be considered in order to correctly interpret the density profiles. One is the amounts of the tetrahedral and octahedral substitutions, which are different in the CH and MMT interlayers, resulting in different total charges in the layers and, therefore, different amounts of cations in the interlayer space. The asymmetry of the clay surfaces that the CH–MM interlayer species are exposed to is another factor that must also be considered.

Foster¹⁹ investigated the effect of all such parameters on swelling of the MMTs. By considering a variety of the MMTs

having different octahedral and tetrahedral substations, as well as different amounts of interlayer cations, he reported that the cation concentration, as well as the tetrahedral substitutions, have little to no effect on the swelling when compared with the octahedral substitutions, which manifested a significant correlation with the swelling volume of the MMT. In fact, both Mg and Fe substitution in the octahedral layer greatly impact clay swelling.

As discussed in Section 3.1, the same behavior is seen in the cases that we have studied. For all the cation types, the CH–CH with full octahedral substitutions swell the least than the other two interlayers. This can be seen by comparing the density profiles in both 1W and 2W hydration states, as shown in Figures 4–6. Such a strong influence is due to the different polarization power of Mg and Fe, compared to Al, which affects polarization of the neighboring atoms and, thus, the entire structure of the clay, changing the interaction energies of all the atoms in the entire CH clay layer.

Comparing the MMT–MMT and CH–CH interlayers, Figure 4 indicates that the preference of the water molecules shifts from hydrating the interlayer Na^+ to forming strong hydrogen bonds with the clay surface. The denser layer substitution of the CH clay is responsible for adsorption of the more polarized water molecules onto the clay surface. The sharper peaks of the water hydrogen near the CH surface, as well as the central water oxygen, can be seen in Figure 4b,c for the 1W hydration state. For the MMT–MMT interlayer, however, the sharper peak is at the central plane where water molecules form hydration shells around part of the Na^+ cations, which results in more swelling of the MMT–MMT interlayer. On the MMT side of the CH–MMT interlayer, the asymmetry of the charges attracts more of the water molecules and Na^+ cations to the CH-surface. Despite the significant differences in the orientations of species in the various interlayers, however, they all depict a monolayer state when 60 water molecules are present in the interlayer with different saturation levels.

The same type of evolution occurs in the cases with 180 water molecules with two distinct hydration layers, 1W and 2W. For the MMT–MMT interlayer, most of the cations are transferred to the central plane to form outer sphere surface complexes (OSSCs) with sharper hydrogen peaks around the central cations, and some inner sphere surface complexes (ISSC) of the cations attached to the clay surface. The OSSCs are formed when ions are distributed over distances 3–6 Å from the clay surface where the cations are hydrated, whereas in the case of the ISSCs the distances are less than 3 Å from the surface where the cation is only partially hydrated, and is directly adsorbed onto the clay surface.³⁸

A few points are worth mentioning here. (i) The increased polarization of water molecules can be understood by the extremely sharper hydrogen peaks at the clay surface. (ii) The central peak of Na^+ in the CH–CH interlayer, which is sharper than that in the MMT–MMT, does not represent more saturated Na^+ cations in the CH–CH. Instead, it is only a result of the “crowded” distribution of water molecules at the clay surface, which forces the cations to migrate to the central plane. To show this better, we should compare the hydrogen peaks in Figure 4d,f. At the clay surface, the hydrogen peaks are at distances 6.3 and 7.4 Å, whereas around the central cations the peaks are at 8.8 and 4.7 Å for the MMT–MMT and CH–CH interlayers, respectively. Therefore, the sharper cation peaks indicate both the tendency of the clay surface to

adsorb more polarized water molecules and the partial saturation of most of the cations. This behavior is consistent with the basal spacings discussed in the previous section. Interestingly, the CH–MMT interlayer manifests a behavior very similar to the MMT–MMT near the MMT surface, and even more similar behavior to the CH–CH interlayer near the CH surface because of the wider basal spacing in the 2W hydration state. This also agrees well with the basal spacings for the CH–MMT that are intermediate between the two cases.

Figure 5 indicates similar behavior for the three interlayers when K^+ is inserted. In general, K^+ perturbs the water network and, relative to Na^+ , is reluctant to fully hydrate.^{39,40} Thus, because of the lower hydration enthalpy of K^+ and its reluctance to hydrate, its peaks in the central plane, shown in Figure 5d, are not as sharp as those in Figure 4d, which is the reason there is a more uniform distribution of K^+ in the interlayers, as indicated by Figure 5. This results directly in less swelling in the K-clay interlayers.

Figure 6 manifests significant differences with the other two cases described so far. Compared with Na^+ and K^+ , Cs^+ has the smallest hydration enthalpy and the largest ionic radius. Thus, as discussed earlier, the global minimum energy of the Cs-clay is reached by the monolayer formation. As mentioned for Figure 3c, the wide range of monolayers for swelling of Cs–CH–CH supports the results in Figure 6c, where the 1W hydration state is not yet stable with 60 water molecules. In addition, because of the larger size of Cs^+ , the adsorption of the cations onto the MMT surface in the CH–MMT interlayer is opposite of the other two cases described so far, where at lower water concentrations the CH surface adsorbs both cations and water molecules. Moreover, in the bilayer state of Cs–MMT–MMT, most of the Cs^+ cations form the ISSC and occupy hexagonal cavities adjacent to the tetrahedral substitution,¹² instead of forming the OSSC, which is due to their low hydration enthalpy; see Figure 6d.

Overall, Figures 4–6 indicate that much stronger hydrogen peaks develop for the monolayer and bilayer of the Na–MMT–MMT, whose height is considerably reduced in the cases of K^+ and Cs^+ . Moreover, as one transitions from the interlayers with Na^+ to those with K^+ and Cs^+ , the cations’ hydration shells become less saturated, resulting in less swelling because of the change in the hydration enthalpy and the size of the cations. Independent of the cation type, in both the 1W and 2W hydration states of all the CH–CH interlayers, sharper water oxygen and hydrogen peaks develop at the clay surface, which are sharper around the central cations in the MMT–MMT interlayers, where the cations are hydrated.

In addition, a comparison of the cations’ distributions in Figures 4–6 indicates that there are two peaks near the CH surface in the 2W state of CH–MMT and CH–CH, corresponding to K^+ and Cs^+ , which represent two types of the ISSCs formed at the CH surfaces. There is, however, only one ISSC peak corresponding to the systems with Na^+ . This agrees well with the study of Underwood et al.,⁴¹ which indicated that weakly hydrating cations form the ISSCs, both above the hexagonal cavities of the clay surface and the basal oxygen atoms. However, strongly hydrated cations, such as sodium, only form ISSCs above the basal oxygen atoms of the clay and, instead, prefer to form OSSCs at high water contents.

Finally, comparing the density profiles of the ML CH–MMT with our previous study on the ML I–MMT,²² we see a significant difference between the distributions of the interlayer

species. For illite with more tetrahedral distributions, most of the cations are adsorbed onto the surface as the ISSCs, independent of the water content in the system. However, as discussed, the dense octahedral substitutions of the CH side of mixed interlayer polarizes the water molecules remarkably, with the ions distribution being a function of the water content of the system. This also explains the differences between the basal spacings of the different cation types.

3.3. Radial Distribution Functions. Figure 7 presents the calculated RDFs $g(r)$ of Na^+ and oxygen in the water

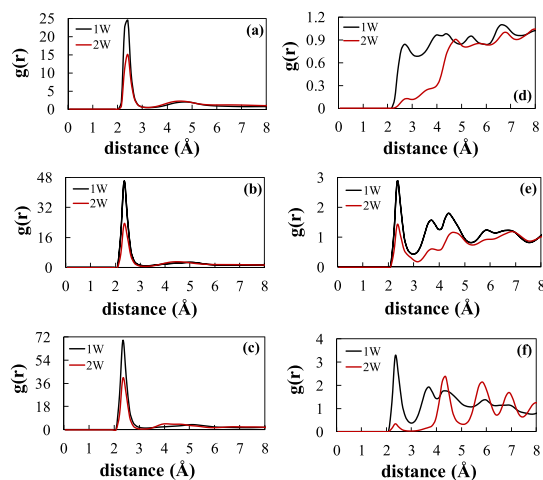


Figure 7. RDF for $\text{Na}-\text{O}_w$ (a–c) and $\text{Na}-\text{O}_s$ (d–f) at 1W (black) and 2W (red); (a,d) $\text{Na} + \text{MMT}-\text{MMT}$; (b,e) $\text{Na} + \text{CH}-\text{MMT}$, and (c,f) $\text{Na} + \text{CH}-\text{CH}$.

molecules, as well as the clay surface oxygen in the three interlayers, namely, $\text{Na}-\text{MMT}-\text{MMT}$, $\text{Na}-\text{CH}-\text{MMT}$, and $\text{Na}-\text{CH}-\text{CH}$. In all the cases, independent of the intensity of the RDFs, the peak location of $r_{\text{O}_w-\text{Na}}$ and $r_{\text{O}_s-\text{Na}}$ is $2.4 \pm 0.1 \text{ \AA}$, which agrees well with the previous studies.^{42,43} The location of the peak reflects the sum of the ionic radii of oxygen and sodium. In all the cases, as water content in the interlayer increases, the height of the peaks corresponding to both $r_{\text{O}_w-\text{Na}}$ and $r_{\text{O}_s-\text{Na}}$ decreases.

The value of $r_{\text{O}_s-\text{Na}}$ confirms the results for the density profiles of sodium and the clay surfaces described earlier. The height of the RDF peak for $\text{Na}-\text{MMT}-\text{MMT}$ decreases considerably in the bilayer state, where sodium cations migrate to the central plane to hydrate. The same significant decrease in the peak height also occurs for the $\text{Na}-\text{CH}-\text{CH}$. As the discussions in the last section indicated, however, this is mostly due to the replacement of the ISSC with Na^+ with water molecules that form strong hydrogen bonds with the clay surface. Therefore, the RDF height of Na^+ decreases at the clay surface, but increases farther in the central plane where they are only partially hydrated, if at all. In addition, in contrast to the other two cases, in the $\text{Na}-\text{CH}-\text{MMT}$ interlayer, Na^+ is exposed to two different clay surfaces and, thus, to the strong charge asymmetry of the interlayer, which is why the RDF peak height does not decrease substantially, hence indicating a persistent ISSC of Na^+ with the surface of the CH side of the interlayer; see Figure 4.

When considering the density profiles and the RDFs, the cations' distributions should be carefully analyzed, because the dense distribution of the cations at the midplane of the CH-

CH interlayer may be mistakenly viewed as hydrated cations, which, as explained earlier, is not the case. Figure 8 presents

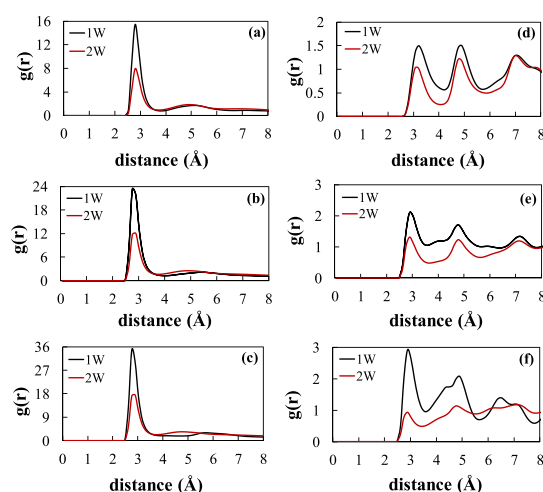


Figure 8. RDF for $\text{K}-\text{O}_w$ (a–c) and $\text{K}-\text{O}_s$ (d–f) at 1W (black) and 2W (red); (a,d) $\text{K} + \text{MMT}-\text{MMT}$; (b,e) $\text{K} + \text{CH}-\text{MMT}$; (c,f) $\text{K} + \text{CH}-\text{CH}$.

the RDFs for K^+ and the three interlayers. The peak location of $r_{\text{O}_w-\text{K}}$ and $r_{\text{O}_s-\text{K}}$ is at $2.8 \pm 0.1 \text{ \AA}$, which agrees with the literature.^{43,44} As expected, because of the lower hydration enthalpy of K^+ compared with $r_{\text{O}_w-\text{Na}}$, $r_{\text{O}_w-\text{K}}$ indicates decreased heights for both the mono- and bilayers. The value of $r_{\text{O}_s-\text{K}}$ indicates that, compared to $\text{Na}-\text{MMT}-\text{MMT}$, there is not significant migration of K^+ to the central plane in $\text{K}-\text{MMT}-\text{MMT}$, as one transitions from the monolayer to the bilayer, hence indicating once again the reluctance of K^+ to hydrate even at higher water contents. Although more of the K^+ migrate to the central plane of the $\text{K}-\text{CH}-\text{CH}$ interlayer, this is again due to the preference of the clay surface for adsorbing more water molecules than K^+ in the CH-CH interlayer, which results in lesser swelling than in the $\text{MMT}-\text{MMT}$ interlayer.

Figure 9 presents the RDFs for the structures containing Cs^+ . The peak of $r_{\text{O}_w-\text{Cs}}$ and $r_{\text{O}_s-\text{Cs}}$ is at $3.2 \pm 0.1 \text{ \AA}$, which agrees with the data in the literature.⁴⁴ The distributions are similar to those for K^+ in the three interlayers. Because of the ionic radius and hydration enthalpy of Cs^+ however, $r_{\text{O}_w-\text{Cs}}$ has the lowest heights among the cations that we study in both the 1W and 2W hydration states, because of which one has a sharper RDF in the bilayer state for both $\text{Cs}-\text{MMT}$ and $\text{Cs}-\text{CH}-\text{CH}$ at $r_{\text{O}_w-\text{Cs}}$ when compared with the other two cations. This indicates that, even in the bilayer state, the Cs^+ are not hydrated and are distributed more near the clay surface than the central planes. This is also consistent with the density profiles in which there is a central peak for both the Na^+ and K^+ bilayers in the CH-CH and MMT-MMT interlayer, which confirms partially and fully hydrated cations in the interlayer regions, respectively. On the other hand, there is no central peak in the bilayer density distribution of Cs^+ and the two interlayers, which again confirms that the global minimum energy of Cs^+ is reached in the monolayer over a wide range of water concentrations.

We point out that, because of the differences in the total negative charge of the CH and MMT clays, different number

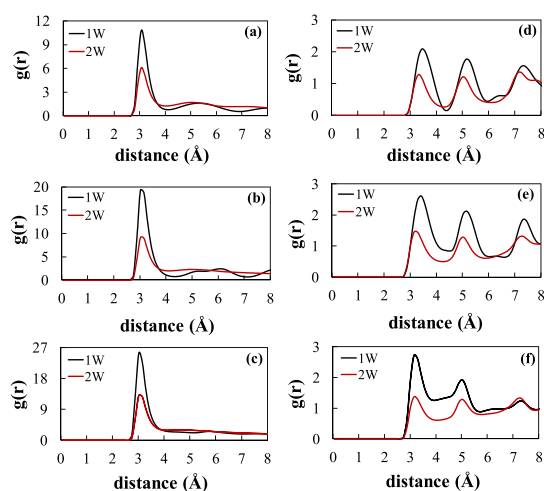


Figure 9. RDF for Cs–O_W (a–c) and Cs–O_S (d–f) at 1W (black) and 2W (red); (a,d) Cs + MMT–MMT; (b,e) Cs + CH–MMT; (c,f) Cs + CH–CH.

of ions exist in each interlayer. In the MMT–MMT, CH–MMT, and CH–CH interlayers a total of 28, 35, and 42 cations are available for neutralizing the charge of the entire structures, which also provides the reasons for the order of $r_{\text{O}_W\text{-cation}}$ in the three interlayers peaks, namely, CH–CH > CH–MMT > MMT–MMT.

4. CONCLUSIONS

Independent of the cation type, sharper peaks for the water oxygen and hydrogen are manifested at the clay surface in both the 1W and 2W hydration states of all the CH–CH interlayers. This indicates the reduced number of water molecules bound to the cations, as well as their increased polarization, having hydrogen bonds with the clay surface. Such a behavior demonstrates how the octahedral substitutions greatly affect clay swelling, whereas the cation concentration, interlayer asymmetry, and tetrahedral substitutions have considerably less influence on the expansion or compression of the clay interlayers.

The hydration enthalpy and size of the cations play significant roles in the swelling of various interlayers. Compared with K⁺ and Na⁺, Cs⁺ hydrates the least, resulting in significant differences in the density profiles of interlayer species and the basal spacing, as well as the RDFs. It should also be pointed out that because of the complexity of the ML structures along with the role of the interlayer cations, the basal spacings, density profiles, and the RDFs should be analyzed simultaneously in order to avoid incorrect interpretation of the overall system's behavior.

Finally, although both illite and CH control swelling of ML clays, there are significant differences between the properties and behavior of I–MMT and CH–MMT. This means that for ML clays, combinations of a variety of parameters with unique properties play a role in their swelling and more studies and investigations should focus on MD simulations with sets of such parameters in order to gain a detailed understanding of the parameters contributing to swelling or shrinking of the other common ML clays.

AUTHOR INFORMATION

Corresponding Author

Muhammad Sahimi – University of Southern California, Los Angeles, Los Angeles, California; orcid.org/0000-0002-8009-542X; Phone: (213) 740-2064; Email: moe@usc.edu

Other Author

Mahsa Rahromostaqim – University of Southern California, Los Angeles, Los Angeles, California

Complete contact information is available at: <https://pubs.acs.org/10.1021/acs.jpcc.9b10919>

Notes

The authors declare no competing financial interest.

ACKNOWLEDGMENTS

This work was supported as part of the Center for Geologic Storage of CO₂, an Energy Frontier Research Center funded by the U.S. Department of Energy, Office of Science, Basic Energy Sciences, under Award DE-SC0012504. The calculations were carried out using 12 nodes (each with 16 processors) of the computer network at the University of Southern California High-Performance Computing Center.

REFERENCES

- (1) Morrow, C. P.; Yazaydin, A. Ö.; Krishnan, M.; Bowers, G. M.; Kalinichev, A. G.; Kirkpatrick, R. J. Structure, Energetics, and Dynamics of Smectite Clay Interlayer Hydration: Molecular Dynamics and Metadynamics Investigation of Na-Hectorite. *J. Phys. Chem. C* **2013**, *117*, 5172–5187.
- (2) Yuan, G. D.; Theng, B. K. G.; Churchman, G. J.; Gates, W. P. Clays and Clay Minerals for Pollution Control. *Handbook of Clay Science*; Developments in Clay Science; Elsevier, 2013; Vol. 5, pp 587–644.
- (3) Lide, D. R. *CRC Handbook of Chemistry and Physics*, 71st ed.; CRC Press: Boca Raton, 1990.
- (4) Anderson, R. L.; Ratcliffe, I.; Greenwell, H. C.; Williams, P. A.; Cliffe, S.; Coveney, P. V. Clay Swelling—a Challenge in the Oilfield. *Earth-Sci. Rev.* **2010**, *98*, 201–216.
- (5) Boek, E. S.; Coveney, P. V.; Skipper, N. T. Monte Carlo Molecular Modeling Studies of Hydrated Li-, Na-, and K-Smectites: Understanding the Role of Potassium as a Clay Swelling Inhibitor. *J. Am. Chem. Soc.* **1995**, *117*, 12608–12617.
- (6) Karaborni, S.; Smit, B.; Heidug, W.; Urai, J.; van Oort, E. The Swelling of Clays: Molecular Simulations of the Hydration of Montmorillonite. *Science* **1996**, *271*, 1102–1104.
- (7) Chávez-Páez, M.; Van Workum, K.; De Pablo, L.; de Pablo, J. J. Monte Carlo Simulations of Wyoming Sodium Montmorillonite Hydrates. *J. Chem. Phys.* **2001**, *114*, 1405–1413.
- (8) Hensen, E. J. M.; Smit, B. Why Clays Swell. *J. Phys. Chem. B* **2002**, *106*, 12664–12667.
- (9) Posner, A.; Quirk, J. P. The Adsorption of Water from Concentrated Electrolyte Solutions by Montmorillonite and Illite. *Proc. R. Soc. Lond. Ser. A Math. Phys. Sci.* **1964**, *278*, 35–56.
- (10) Denis, J. H.; Keall, M. J.; Hall, P. L.; Meeten, G. H. Influence of Potassium Concentration on the Swelling and Compaction of Mixed (Na, K) Ion-Exchanged Montmorillonite. *Clay Miner.* **1991**, *26*, 255–268.
- (11) Liu, X.-D.; Lu, X.-C. A Thermodynamic Understanding of Clay-Swelling Inhibition by Potassium Ions. *Angew. Chem., Int. Ed.* **2006**, *45*, 6300–6303.
- (12) Smith, D. E. Molecular Computer Simulations of the Swelling Properties and Interlayer Structure of Cesium Montmorillonite. *Langmuir* **1998**, *14*, 5959–5967.

- (13) Mooney, R. W.; Keenan, A. G.; Wood, L. A. Adsorption of Water Vapor by Montmorillonite. II. Effect of Exchangeable Ions and Lattice Swelling as Measured by X-Ray Diffraction. *J. Am. Chem. Soc.* **1952**, *74*, 1371–1374.
- (14) Young, D. A.; Smith, D. E. Simulations of Clay Mineral Swelling and Hydration: Dependence Upon Interlayer Ion Size and Charge. *J. Phys. Chem. B* **2000**, *104*, 9163–9170.
- (15) Norrish, K. The Swelling of Montmorillonite. *Discuss. Faraday Soc.* **1954**, *18*, 120–134.
- (16) Tambach, T. J.; Hensen, E. J. M.; Smit, B. Molecular Simulations of Swelling Clay Minerals. *J. Phys. Chem. B* **2004**, *108*, 7586–7596.
- (17) Smith, D. E.; Wang, Y.; Whitley, H. D. Molecular Simulations of Hydration and Swelling in Clay Minerals. *Fluid Phase Equilib.* **2004**, *222–223*, 189–194.
- (18) Whitley, H. D.; Smith, D. E. Free Energy, Energy, and Entropy of Swelling in Cs-, Na-, and Sr-Montmorillonite Clays. *J. Chem. Phys.* **2004**, *120*, 5387–5395.
- (19) Foster, M. D. Geochemical Studies of Clay Minerals: II—Relation between Ionic Substitution and Swelling in Montmorillonites. *American Mineralogist* **1953**, *38*, 994–1006.
- (20) Weaver, C. E. The Distribution and Identification of Mixed-Layer Clays in Sedimentary Rocks. *American Mineralogist* **1956**, *41*, 202–221.
- (21) Rahromostaqim, M.; Sahimi, M. Molecular Dynamics Simulation of Hydration and Swelling of Mixed-Layer Clays in the Presence of Carbon Dioxide. *J. Phys. Chem. C* **2019**, *123*, 4243–4255.
- (22) Rahromostaqim, M.; Sahimi, M. Molecular Dynamics Simulation of Hydration and Swelling of Mixed-Layer Clays. *J. Phys. Chem. C* **2018**, *122*, 14631–14639.
- (23) Chapter 8 Mixed-Layer Clay Minerals. In *Developments in Sedimentology*; Weaver, C. E., Pollard, L. D., Eds.; Elsevier, 1973; Vol. 15, pp 107–118.
- (24) Meunier, A.; Inoue, A.; Beaufort, D. Chemigraphic Analysis of Trioctahedral Smectite-to-Chlorite Conversion Series from the Ohyu Caldera, Japan. *Clays Clay Miner.* **1991**, *39*, 409–415.
- (25) Weaver, C. E.; Pollard, L. D. *The Chemistry of Clay Minerals*; Elsevier, 2011; Vol. 15.
- (26) Fu, M. H.; Zhang, Z.; Low, P. Changes in the Properties of a Montmorillonite-Water System During the Adsorption and Desorption of Water: Hysteresis. *Clays Clay Miner.* **1990**, *38*, 485–492.
- (27) Slade, P. G.; Quirk, J.; Norrish, K. Crystalline Swelling of Smectite Samples in Concentrated NaCl Solutions in Relation to Layer Charge. *Clays Clay Miner.* **1991**, *39*, 234–238.
- (28) Greathouse, J.; Sposito, G. Monte Carlo and Molecular Dynamics Studies of Interlayer Structure in Li (H₂O) 3- Smectites. *J. Phys. Chem. B* **1998**, *102*, 2406–2414.
- (29) Liu, X.; Lu, X.; Wang, R.; Zhou, H. Effects of Layer-Charge Distribution on the Thermodynamic and Microscopic Properties of Cs-Smectite. *Geochim. Cosmochim. Acta* **2008**, *72*, 1837–1847.
- (30) Teich-McGoldrick, S. L.; Greathouse, J. A.; Jové-Colón, C. F.; Cygan, R. T. Swelling Properties of Montmorillonite and Beidellite Clay Minerals from Molecular Simulation: Comparison of Temperature, Interlayer Cation, and Charge Location Effects. *J. Phys. Chem. C* **2015**, *119*, 20880–20891.
- (31) Plimpton, S. Fast Parallel Algorithms for Short-Range Molecular Dynamics. *J. Comput. Phys.* **1995**, *117*, 1–19.
- (32) Cygan, R. T.; Liang, J.-J.; Kalinichev, A. G. Molecular Models of Hydroxide, Oxyhydroxide, and Clay Phases and the Development of a General Force Field. *J. Phys. Chem. B* **2004**, *108*, 1255–1266.
- (33) Degrève, L.; Vecchi, S. M.; Junior, C. Q. The Hydration Structure of the Na⁺ and K⁺ Ions and the Selectivity of Their Ionic Channels. *Biochim. Biophys. Acta, Bioenerg.* **1996**, *1274*, 149–156.
- (34) Hensen, E. J. M.; Tambach, T. J.; Blik, A.; Smit, B. Adsorption Isotherms of Water in Li-, Na-, and K-Montmorillonite by Molecular Simulation. *J. Chem. Phys.* **2001**, *115*, 3322–3329.
- (35) Tao, L.; Xiao-Feng, T.; Yu, Z.; Tao, G. Swelling of K⁺, Na⁺ and Ca²⁺-Montmorillonites and Hydration of Interlayer Cations: A Molecular Dynamics Simulation. *Chin. Phys. B* **2010**, *19*, 109101.
- (36) Marry, V.; Turq, P.; Cartailier, T.; Levesque, D. Microscopic Simulation of Structure and Dynamics of Water and Counterions in a Monohydrated Montmorillonite. *J. Chem. Phys.* **2002**, *117*, 3454–3463.
- (37) Ngouana W, B. F.; Kalinichev, A. G. Structural Arrangements of Isomorphous Substitutions in Smectites: Molecular Simulation of the Swelling Properties, Interlayer Structure, and Dynamics of Hydrated Cs-Montmorillonite Revisited with New Clay Models. *J. Phys. Chem. C* **2014**, *118*, 12758–12773.
- (38) Lammers, L. N.; Bourg, I. C.; Okumura, M.; Kolluri, K.; Sposito, G.; Machida, M. Molecular Dynamics Simulations of Cesium Adsorption on Illite Nanoparticles. *J. Colloid Interface Sci.* **2017**, *490*, 608–620.
- (39) Boek, E. S. Molecular Dynamics Simulations of Interlayer Structure and Mobility in Hydrated Li-, Na- and K-Montmorillonite Clays. *Mol. Phys.* **2014**, *112*, 1472–1483.
- (40) Chang, F.-R. C.; Skipper, N. T.; Sposito, G. Monte Carlo and Molecular Dynamics Simulations of Electrical Double-Layer Structure in Potassium-Montmorillonite Hydrates. *Langmuir* **1998**, *14*, 1201–1207.
- (41) Underwood, T.; Erastova, V.; Greenwell, H. C. Ion Adsorption at Clay-Mineral Surfaces: The Hofmeister Series for Hydrated Smectite Minerals. *Clays Clay Miner.* **2016**, *64*, 472–487.
- (42) Chang, F.-R. C.; Skipper, N.; Refson, K.; Greathouse, J. A.; Sposito, G. Interlayer Molecular Structure and Dynamics in Li-, Na-, and K-Montmorillonite-Water Systems. *ACS Symposium Series*; ACS Publications, 1998.
- (43) Boulet, P.; Coveney, P. V.; Stackhouse, S. Simulation of Hydrated Li⁺, Na⁺ and K⁺-Montmorillonite/Polymer Nanocomposites Using Large-Scale Molecular Dynamics. *Chem. Phys. Lett.* **2004**, *389*, 261–267.
- (44) Kosakowski, G.; Churakov, S. V.; Thoenen, T. Diffusion of Na and Cs in Montmorillonite. *Clays Clay Miner.* **2008**, *56*, 190–206.